Energy for Sustainable Development 37 (2017) 1–9

Contents lists available at ScienceDirect

Energy for Sustainable Development

# Semi-industrial drying of vegetables using an array of large solar air collectors

Miguel Condorí *, Gonzalo Duran, Ricardo Echazú, Fabiana Altobelli

*Instituto de Investigaciones en Energía no Convencional, Universidad Nacional de Salta, CONICET, Av. Bolivia 5150, A4408FVY Salta, Argentina*

ARTICLE INFO

*Article history:*
Received 21 June 2015
Revised 18 October 2016
Accepted 29 November 2016
Available online xxxx

*Keywords:*
Solar dryer
Drying of vegetables
Air solar collector
Clean energy project

ABSTRACT

The design, structure, and evaluation of an indirect solar tunnel dryer are presented. This dryer corresponds to the air forced convection type. Two similar solar dryers were built and tested with vegetables on an industrial scale in Huacalera, northern Argentina, and operated by a cooperative of small agricultural producers. Each dryer consisted of a tunnel chamber of 450 kg load capacity and a bank of 10 solar collectors of 92 $m^2$. The bank of large solar collectors allowed temperatures in the drying chamber above 50 °C for 6 h a day, mixing with ambient air to produce the correct temperature for drying vegetables. A maximum rank of outlet temperatures of 80–90 °C and temperature differences of 50–60 °C were obtained with minimum air flow of 0.06 kg/s and without load. The dryers were operated with different vegetables, obtaining e.g. dried slicing onion with final moisture content 0.09 in approximately 16 h of sun. The optimum point of the collector efficiency was determined with airflow of 0.4 kg/s, however, lower than 0.23 kg/s airflow is needed to obtain outlet temperatures above 50 °C. A financial evaluation of the dryer was also performed as a clean energy project, reflecting that the investment return rate of the device is 13 months. In this scenario NPV improves in a 438% compared with the conventional scenario and SNPV is suitable only in the case of solar dryer. Solar drying at semi-industrial scale is feasible with the proposed technology due to the gusts of wind and the day-night thermal amplitude of Huacalera.



## Introduction

Regions of Northern Argentina lack adequate access to conventional energy sources. In these places the main source of subsistence is the family agriculture, with small producer cooperatives that achieve significant production volumes. The local production is entirely destined for the fresh market, thus, the solar drying can be a tool for adding value to this activity, allowing the access to other markets. Numerous successful experiences exist worldwide in relation to solar drying technology with different agricultural products (Ringeisen et al., 2014; Stiling et al., 2012; Soponronnarit, 1995).

Even though there is a lot of work done in solar drying technology, solar dryer on an industrial scale has not been sufficiently studied and further research to optimize appropriate solar dryers is required. This application requires large banks of solar collectors to ensure energy supply (VijayaVenkataRamana et al., 2012; Sharma et al., 2009). The main aspects to achieve are to minimize the drying time and satisfy the product's quality requirement. The dryer production must be optimized to achieve the investment return rate. It is important to keep the drying rate as high as possible and assure a continuous production, since the final income is directly related to the drying costs by kilogram of dried product. Consequently, hybrid solar dryers with auxiliary heating systems and forced air circulation are normally used.

In 2007, a regional project including the construction of two industrial solar dryers started in Huacalera. The main objective pursued by the project was the improvement in the living conditions of the local population, generating sustainable added value to the production. This project, involved the participation of local NGO's with funding from the Spanish Agency for International Cooperation.

The town of Huacalera (latitude 23° 26′ S; longitude 65° 21′ W), is placed in Quebrada de Humahuaca at north of Argentina, at a height of 2462 m above the sea level. Crossed by the Capricorn Tropic, this zone was declared as natural and cultural heritage of humanity by UNESCO. The climate is arid with an average annual temperature of 13 °C and an annual average rainfall of 121 mm concentrated in December to March. The annual average wind speed is 5 m/s with gusts of intensity. There is no adequate supply of conventional energy, however, the solar resource is abundant (Reghini et al., 2005; Altobelli et al., 2014; Belmonte et al., 2009). The heliophany and the solar radiation level of this region are considered among the highest in the world. However, open sun drying is hard to be implemented due to the temperature amplitude, the strong winds and the risks of dust pollution.

Two similar solar dryers were built in Huacalera. A bank of solar collectors was used as air heating system, having the design criteria of provide temperatures above 50 °C during 6 or 7 h per day, from the total of

* Corresponding author.
*E-mail address:* miguel.angel.condori@gmail.com (M. Condorí).

http://dx.doi.org/10.1016/j.esd.2016.11.004
0973-0826/

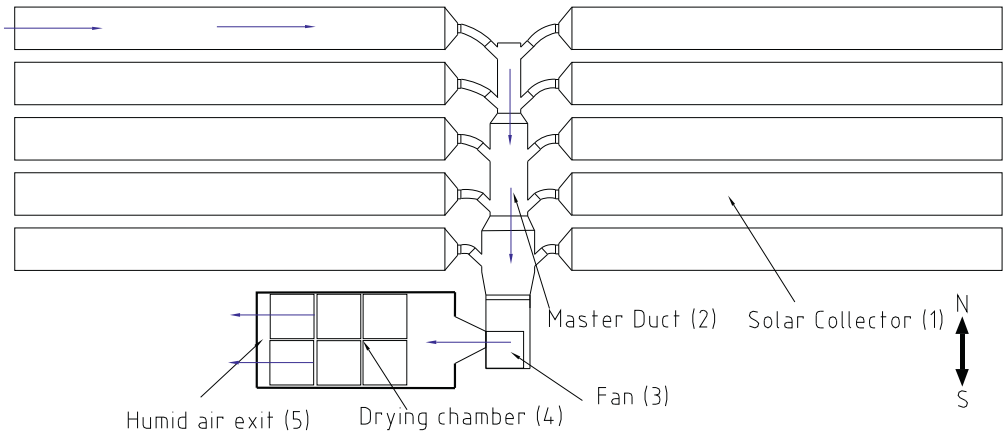


**Fig. 1.** Solar dryer plant view. The main parts are highlighted and air circulation is shown in blue arrows. (For interpretation of the references to color in this figure legend, the reader is referred to the web version of this article.)

sunny hours. It is necessary to perform a mix with ambient air to prevent product burning. As a result, the dryer allow completing the drying in one or two sunny days, depending on the product conditions. These dryers can be classified as indirect according to the relation with sunlight, and as a tunnel type of semi-industrial scale if load capacity is considered ( Mujundar, 1987; Duffie and Beckman, 2006).

## Solar dryer construction

The dryers were constructed by local labour with basic training in blacksmithing. A plant schema of the dryer is shown in Fig. 1 and photography in Fig. 2. The main parts are the collector array, a master duct, fan cabinet and drying chamber. For operating reasons, the drying chambers were faced by the output doors, leaving a corridor in the middle to allow the carts movement. A first bank of collectors was placed north of the chamber, while a second bank of collectors was placed at the south side of the other chamber, but facing north and far enough from the chamber shadows, taken the average winter day as reference. The collector array was built with 10 solar air collectors, 5 on each side of the master duct, and including an electric fan to force the air circulation. Inside the drying chamber the product was distributed on six carts of 15 trays each.

The ambient air enters the solar collectors forced by the fan, and passes through them increasing its temperature, (1). An air filter of synthetic fiber is placed at the inlet of each collector to prevent the dust access. The master duct collects all contributions of collectors and it also works as another solar collector, (2). Before the fan, there is also a metal filter to remove particles, (3). The air is then forced into the drying chamber where it is laden with moisture, (4). All the humid air is discarded through two windows placed at the entrance gate of fresh product, (5). These windows also have air filters to prevent dust or insects entrance.

All collectors and master duct work in low air pressure while the drying chamber makes it at over pressure. The product is placed on trays, which are stacked on six carts. The carts are moved manually inside the chamber in the counter current direction of the air flow, producing a drying gradient along the tunnel. That is, the product located near the entrance of warm air has lower water content than that placed in the humid air exit. The carts with fresh products are entered into the chamber by this last side, and moved forward while the dried product is removed from a door place alongside the inlet air.

The solar collectors were separated 0.4 m to avoid shading between them and to allow operator transit. They are faced north, where five vertical supports, regularly spaced along the collector, are used to fit the slope. One of the long sides of the collectors is attached to these vertical supports while the other side rests on the floor. The supports consist of square structural pipes of 40 mm side and 0.7 m long; those were founded on the ground by concrete and were united to the external racks of the collectors by screws. Since only one side of the collectors was fixed, the collector slope can be changed seasonally according to the midday sun altitude, improving the direct solar radiation on the collector plane.

Large air solar collectors were used in the design of the dryers. These collectors are an improved version of the solar collector single pass with suspended flat plate, which allows the passage of air flow above and below the absorber (Ekechukwu and Norton, 1999). In this study, a

**Fig. 2.** Photograph of solar dryer. The collector array, fan cabinet and drying chamber are shown.

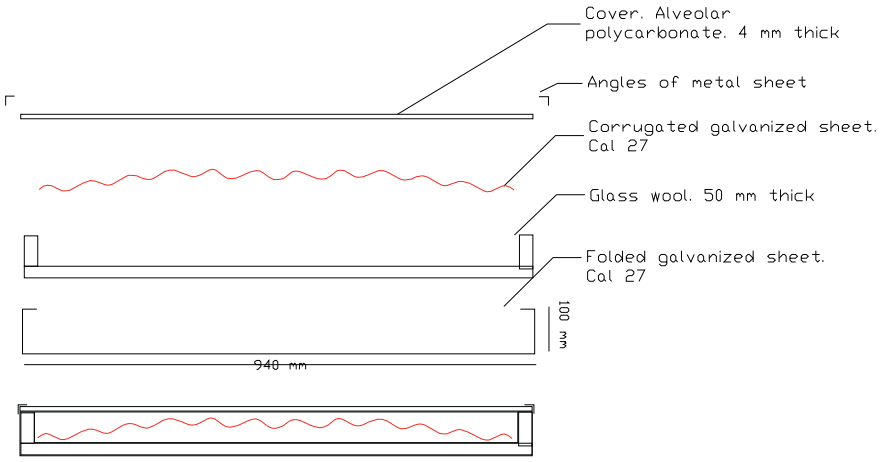


**Fig. 3.** Plane parts of cross section of the solar air collector of 0.94 m width, 9.76 m long and 0.1 m high.

corrugated sheet was used as absorber plate to enhance the convective contact area and also a larger area of 9.17 $m^2$, since the temperatures required improving the drying rate (Condorí et al., 2006).

The constructive aspects of the collector are presented with sufficient details as to be replicated. A frontal cutting plane of the air solar collector is shown in Fig. 3. Each solar collector is a box of 0.94 m width, 9.76 m long and 0.1 m high. The external box was built with four overlapped galvanized iron sheets of 2.44 m by 1.22 m each one. These boxes are constructed by folding inwards the long sides of the sheets 10 cm, 2 cm, and 2 cm. Each collector has five external U shaped racks constructed with structural pipes of 4 cm by 2 cm. The galvanized sheet boxes were placed in the racks and attached with screws to these structures. The box inner surfaces were insulated with glass wool of 5 cm thick with reinforced aluminum foil on the upper face. A corrugated galvanized sheet of 9.76 m long, painted in matte black on the upper face, was used as an absorber plate. This sheet was separated from the bottom of the collector in order to allow the air circulation above and below it. The top cover was transparent alveolar polycarbonate of 4 mm thick linked by a T-connector polycarbonate to reach the total longitude. Silicone sealant was placed between the polycarbonate and the galvanized box. Finally, 2 cm side sheet angles were placed over the top cover and fitted to the box with screws.

Each collector was connected to the master duct trough reduction hoods. These hoods were also built in galvanized sheet, going from a rectangular section to a circular one of 0.2 m diameter. Flexible aluminum pipes were used to connect each reduction hoods to 45° couplings placed in the master duct. A floodgate to control the airflow was placed in the circular section of each reduction. The whole connection set was thermally isolated with glass wool of 5 cm thick and aluminum membrane above.

The master duct was built as another solar collector. This was 7 m long and consisted of three rectangular boxes of sections 0.15 $m^2$, 0.32 $m^2$, and 0.6 $m^2$ respectively, to avoid the rising of pressure drop. Each section was built using galvanized sheets with insulated glass wool of 5 cm thick between them. The internal sheet was painted in matte black and a transparent polycarbonate sheet of 4 mm thick was used as cover.

The fan was placed in a thermally insulated cabinet of 1.5 m long and square section of 1 m sides. A column of 4 stainless steel filters of 0.5 m side each was installed 30 cm before the fan. A centrifugal blower was used, in order to force the airflow, connected to a single phase electric engine of 1 hp and 1500 rpm. The connection between the fan cabinet to the drying chamber was made through a diffuser of 1 $m^2$ section at the end.

The drying chamber was a tunnel of 1.85 m high, 4.5 m long and 2.15 m wide. The chamber was covered with corrugated galvanized sheets, and insulation of glass wool was included between the internal and external sheets. The tunnel structure was fixed to the floor using large screws and rubber weather stripping was installed to prevent air leakage. The floor was built using polystyrene expanded plates of 5 cm thick as thermal insulation. Above this, a reinforced concrete folder of 5 cm thick was placed. The gate to remove the dried product was a sheet of 1.1 m by 1.85 m, while the gate where the fresh product is entered was two similar sheets. Two windows of 0.5 $m^2$ each were placed at the top of the input gates. The chamber has a thermally isolated gable roof of corrugated galvanized sheets.

Two rows of 3 carts were placed into the drying chamber. Each cart had 1.80 m height and carried 15 trays of 1 $m^2$ each. The frame of the trays was constructed of structural iron pipe of 2 cm thick and then covered with thin stainless steel plate. Plastic mesh was used as grid to allow air circulation. The load density of each tray was near to 5 kg/$m^2$ of fresh pepper, i.e. approximately 75 kg by carts. For vegetables with leaves, the load density is reduced approximately by half. An image of the carts and trays is shown in Fig. 4.

**Fig. 4.** Loading door of drying chamber, with carts and trays inside the chamber.

## Dryer and collector testing

A series of tests to determine the dryer behavior were carried out. The variables: ambient temperature, collector output temperature, chamber temperatures, relative humidity, total solar radiation, and wind speed, were recorded simultaneously using a data logger. The measurements were recorded and stored using a Campbell Scientific data logger Model CR 32X. A solid state multiplexer Campbell Scientific AM25T was attached to it allowing the recording of 25 temperature channels. A Kipp&Zonen Pyranometer CM3 was used for solar radiation. A hot wire TSI Model 8345 Velocicalc was used for air speed. The relative humidity was measured with Vaisala HMP25A sensors. The temperatures were measured with calibrated type K thermocouples, protected with aluminum reflective cylinders. The weight change of the product samples was followed with a precision weighing scale Ohaus Scout Pro 400.

*Tests with unloaded chamber*

The first tests were performed with the drying chamber unloaded, in order to verify the performance of the solar heating system.

The air temperatures for the solar collector using lower air flow, an average air flow of 0.06 kg/s, are presented in Fig. 5 for four consecutive days. These measures correspond to one of the collectors placed east from the master duct. The last two days were partially clouded; however, similar conditions were obtained for temperature rise at noon. The input temperature was close to the ambient temperature, in the middle of the collector it was between 40 and 50 °C, and in the output between 80 and 90 °C. The temperature gain at noon is around 50–60 °C. At night, temperatures decreased to 5 °C showing the wide thermal amplitude suffered by the collector, especially in the polycarbonate cover. As the inlet temperature is the ambient temperature it is not mainly affected by cloudiness. But the solar collector has not high thermal inertia; hence the output temperature is so variable with the solar radiation intensity.

Fig. 6 shows the ambient temperature and total solar radiation on horizontal surface for a sunny day of May. The maximum ambient temperature for this day was 28 °C at solar noon and the minimum 5 °C at night, reflecting a day–night amplitude of about 23 °C which is a local characteristic. The maximum solar radiation on horizontal surface was approximately 800 W/m$^2$. The drying plant of Huacalera is located between two mountain ranges, the Quebrada de Humahuaca, which stretches from north to south; therefore, the sunrise on the solar collector was at 08:00 and the sunset at 18:00, leaving 10 h of effective solar light.

The airflow temperatures along the East collector are shown in Fig. 7. Since the collector works in open loop, the inlet temperature has been similar to the ambient temperature. Air velocities were measured above and below the absorber plate in the outlet, being the average air flow 0.06 kg/s during the tests. The air temperature sensor in half

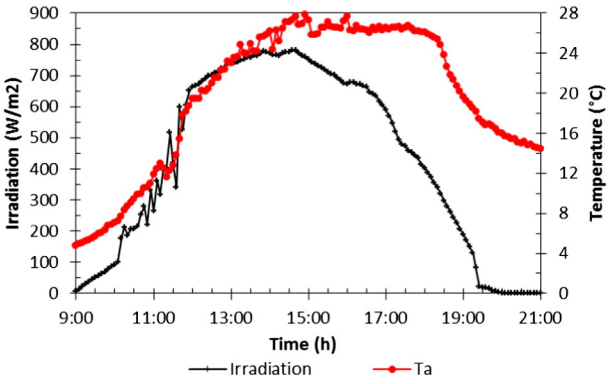


**Fig. 6.** Total solar radiation on the horizontal surface and ambient temperature measured in 3rd May in Huacalera.

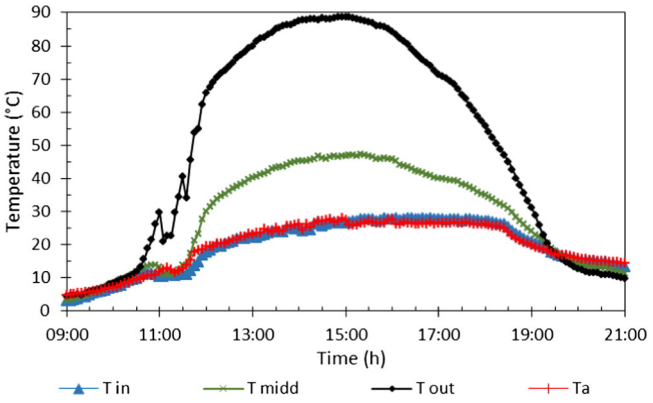


**Fig. 7.** Temperatures measured in the ambient and input, half and output of East collector for the 3rd May.

of the collector was located below the absorber plate, measuring 48 °C at solar noon. The outlet temperatures of the collector were above 50 °C during about 6 1/2 h, between 10:40 and 17:10, with a maximum close to 90 °C at noon. The output temperatures highlight the fact that the collector might provide these temperatures even on cloudy days, during 6–7 h. Even though these temperatures are too high to drying applications, it is possible to reduce them by mixing with ambient air. This result is due to the fact that low air flow was used and also due to the proper collector performance with diffuse radiation.

The airflow temperatures at the exit of the collector, master duct, and drying chamber, are shown in Fig. 8. At solar noon, ambient air was warmed from 28 °C to 88 °C. The temperature decreased to 80 °C in the master duct and to 75 °C in the drying chamber, reflecting the existence of avoidable thermal losses. Considering a temperature

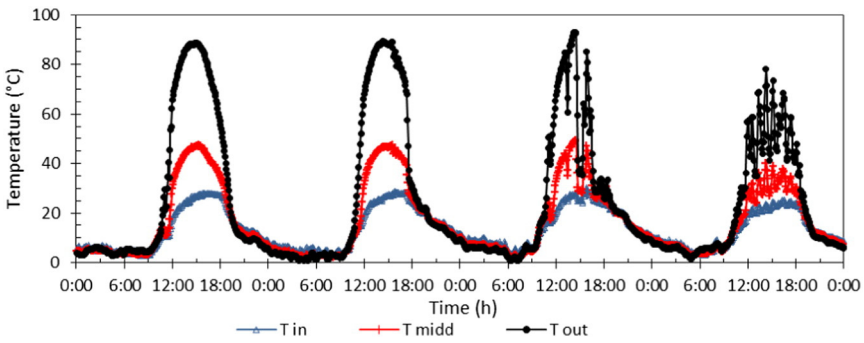


**Fig. 5.** Four consecutive days of May. Inlet, middle and outlet temperatures taken from the East collector.

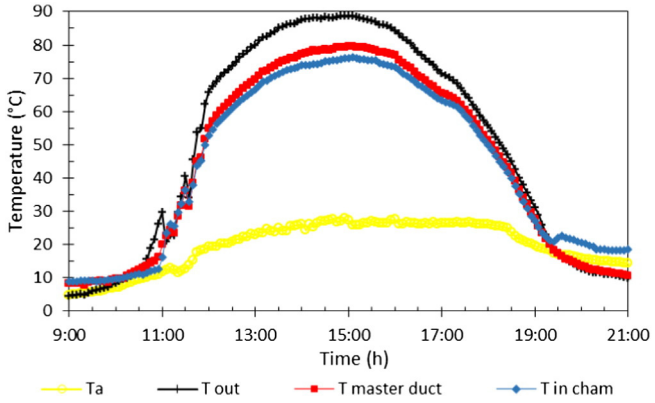


**Fig. 8.** Ambient temperature and temperatures at the outlet collector, master duct and drying chamber.

difference of 60 °C between input and output air of the collector, the peak useful heat of each collector was 3.6 kW. In the drying chamber, temperatures above 50 °C were reached during about 6 h.

The efficiency of the collector Eq. (1), depending on the difference between the input and output temperatures, divided by the solar radiation on the collector plane are shown in Fig. 9.

$$\eta = \frac{\dot{m}C_p(T_{out} - T_a)}{A_c G_T} \quad (1)$$

where $\dot{m}$ is the mass air flow, $C_p$ is the air heat capacity, $T_{out}$ is the output temperature of collector and $T_a$ is the input temperature, i.e. the ambient temperature. $A_C$ is the collector area and $G_T$ is the solar radiation on collector surface (Duffie and Beckman, 2006).

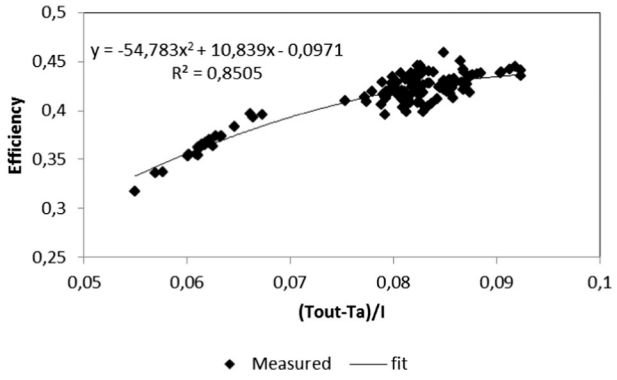


**Fig. 9.** Efficiency of collector depending on the difference between the inlet and outlet temperatures divided by the solar radiation on the collector plane. Curve fitting in solid line.

The measured data was obtained from experiences in Huacalera from May 3rd to 11th, taking values around the solar midday. Because the input temperature was the ambient temperature, the performance curve of collector cannot be shown in a conventional way. Instead, using the output temperature it produces a positive slope. It is noted that while a linear fitting can be used (R2 = 0.80), a slight improvement was obtained using a second order polynomial curve, R2 = 0.85.

*Tests with loaded chamber*

Simple screens were placed around the carts so the airflow was forced to go through the trays improving the air distribution. The airspeed was measured in the cross section of 3.6 $m^2$ of the drying chamber and a more uniform air flow distribution could be observed. The range of the air speed inside the chamber was between 0.13 m/s and 0.23 m/s with an average speed of 1.7 m/s, and a mass air flow of about 0.65 kg/s.

As regards the temperature of airflow, it also showed a uniform distribution, being the difference between measured points of only about 1 °C. During solar noon the average temperature at the chamber's exit was around 54 °C, showing that the air leaving the chamber still has available energy. In an enthalpy constant process, the air could leave the chamber with a lower temperature, according to psychrometric charts.

The dryer was also tested loaded with products. In Fig. 10, the evolution of temperatures during a drying cycle of onion for May is shown. On the second day, ambient temperature below 0 °C was recorded, whereas at noon this exceeded the 20 °C. The air temperature from the collectors was above 40 °C for 6 h or more. The collector air was mixed with ambient air and the peaks of temperature do not cause damages to the product in brief periods. The air temperature at the outlet of the chamber is declined near to 40 °C due to energy delivered to the product. The third day, the outlet temperature of the drying chamber was 55 °C due to the low moisture content of products. These values showed the existence of an untapped potential of heat in the hours around noon. The nighttime temperatures inside the chamber were 5 °C or more above the ambient temperature due to the thermal insulation and the heat stored in the product.

Onion is one of the most important crops of the Quebrada de Humahuaca. For drying purposes, it was peeled, washed, cut into slices about 2–3 mm, and finally treated with hypochlorite and loaded in the trays with a density of 3 kg/$m^2$. During drying, the onion slices surface was darkened in some trays. This was detected when the temperature was too high, above 50 °C. Drying curves in dry basis (X) versus time were plotted, being X defined in Eq. (2).

$$X = \frac{m - m_s}{m_s} \quad (2)$$

where $m$ is the mass of the product sample and $m_s$ its dried mass. In Fig. 11, the obtained curve for onion is shown. The samples were dried

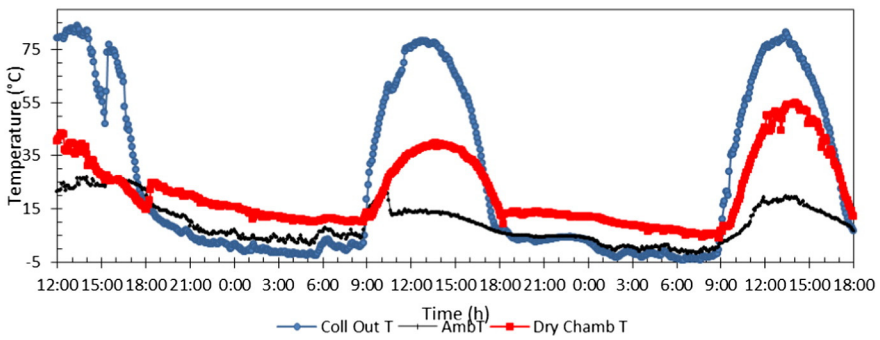


**Fig. 10.** Ambient temperature, the output temperature of the collector and drying chamber during drying of onion.

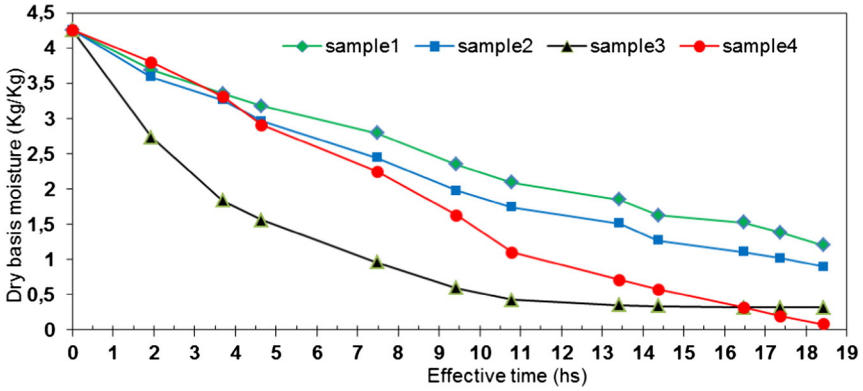


**Fig. 11.** Drying curves of onion cut in 3 mm thick using the effective solar hours. The different samples were placed along the drying chamber, being the 3 and 4 the nearest to the inlet of heat air from collectors.

during 16 h of effective operation in average, which are approximately one day and a half of sun. The two samples located in carts near the discharge door had higher moisture content and were removed the next day, providing a continuous daily production.

In other tests, the dryer was loaded at different times with grated carrot, sliced onion, diced garlic and several types of leaves like spinach, leeks, celery, chard and parsley (Echazú et al., 2007). Table 1 shows a summary of the drying of these vegetables, with the pretreatments and load density used in each case. The results obtained were very good both in drying time as in the final product's quality. Furthermore, the products were used to produce cream dehydrated soups with Andean ingredients such as quinoa, kollallaw (yellow corn), kulli (purple corn). For leaf type vegetables the drying time was about a sunny day, but for vegetables with stems or tubers one and a half day was needed. For every product the warm air from the collectors was mixed with ambient air when the burned temperature condition could be achieved.

*Test with a solar collector prototype*

Tests to determine the performance of a solar collector prototype of 9.76 m were carried out in the experimental field of INENCO, National University of Salta (latitude 24° 48′ S, longitude 65° 25′ W). For this purpose, the following variables were measured: ambient temperature, total solar radiation on collector plane, the air temperature at the entrance, center and outlet of the collector, and also both upper and lower the absorber. Moreover, the air flow speed was manually measured in the cross sections at the input and output of the collector. A centrifugal fan of 1/4 hp was placed in the input to force the air through the collector, and an articulated air register was placed in the output to vary the air flow.

**Table 1**
Charge density per square meter of tray and initial and final moisture content of different vegetables.

| Product | Load density (kg/m2) | Pretreatment | Final moisture content dry basis (%) |
|---|---|---|---|
| Carrot | 5–6 | Grated | 3.0 |
| Red pepper | 4–5 | Slicing | 2.5 |
| Rucula | 3 | Chopped | 4.8 |
| Cabbagge | 4 | Chopped | 2.5 |
| Pear | 4–5 | Slicing | 7.1 |
| Leek | 4–6 | Chopped | 6.3 |
| Fig | 4–5 | Whole | 20.0 |
| Bean | 5–6 | Whole | 6.6 |
| Onion | 3 | Slicing | 7.7 |
| Banana | 5–6 | Slicing | 9.0 |
| Chard | 2 | Chopped | 4.5 |
| Celery | 2–3 | Chopped | 4.8 |
| Spinach | 2–3 | Chopped | 4.7 |
| Apple | 4–5 | Slicing | 5.5 |
| Parsley | 3 | Chopped | 4.2 |
| Garlic | 3 | Slicing | 6.5 |

The tests were usually carried out from 11:00 to 15:00 h (local time) that is 4 h around solar noon, orienting the collector plane with normal incidence of solar radiation at noon. All the measurements were performed in fourteen days distribute in June and December, using only clear sunny days. Calibrated thermocouples type K, with protection against IR, were used. Solar radiation was recorded with a solar pyranometer LICOR Li - 200. These sensors were connected to a data logger Nudam 425. The air flow speed was measured in several places in the inlet and outlet sections of the collector, and then the average of these values was used.

As previously mentioned, the batch of data had 14 days, 9 corresponding to June and 5 to December. Due to the big amount of information generated, data are presented in the next graphics as average, minimum and maximum values for this time interval. Table 2 shows a summary with the average air flow, average efficiency, difference of temperature and ambient temperature for each day. The temperature difference (Tout-Tin), was estimated as the average temperatures measured above and below of the absorber as shown in the Eq. (3).

$$(T_{out} - T_{in}) = \frac{1}{2}\left[(T_{o,arr} + T_{o,aba}) - (T_{i,arr} + T_{i,aba})\right] \quad (3)$$

In this equation, To,arr and Ti,arr are the temperatures measured in the output and input of collector but in the upper channel. Similarly, Ti,aba and To,aba are the temperatures measured in the lower channel.

Measured airflow temperatures at the outlet of the collector are shown in Fig. 12, this is an average between the temperatures above and below of the absorber. The dots indicate the mean value, while the dashes indicate maximum and minimum values, as appropriate. In addition, the abscissa axis indicate the average air flow used in the collector during each test. The maximum outlet temperature was 90 °C, obtained with the lower air flow 0.07 kg/s. In the case of the maximum air flow 0.13 kg/s, the maximum temperature obtained was 55 °C, with an average of 45 °C. If the lower value of airflow does not take account, the rank of the average temperature for all cases was between 35 °C and 45 °C.

The differences of temperature between the output and input of the collector, estimated according to Eq. (3), are shown in Fig. 13. These average differences have values ranging from 10 °C to 45 °C, for the various flow rates tested. The extreme values obtained during the last day correspond to the lowest air flow, 0.07 kg/s.

The useful power of the collector was estimated using the following equation:

$$Q_u = \dot{m} C_p (T_{out} - T_{in}) \quad (4)$$

**Table 2**
Air flow, efficiency, difference of temperature and ambient temperature.

| Day no | Date | Flow (kg/s) | Avg. $\eta$ | $(T_o - T_i)$ Max (°C) | $(T_o - T_i)$ Min (°C) | $(T_o - T_i)$ Med (°C) | $T_{amb}$ Max (°C) | $T_{amb}$ Min (°C) | $T_{amb}$ Med (°C) |
|---|---|---|---|---|---|---|---|---|---|
| 1 | 4–6 | 0.13 | 0.47 | 30.54 | 5.61 | 20.05 | 21.40 | 12.20 | 18.33 |
| 2 | 5–6 | 0.11 | 0.41 | 27.85 | 20.95 | 25.30 | 24.00 | 13.00 | 20.14 |
| 3 | 6–6 | 0.24 | 0.52 | 18.84 | 0.00 | 15.09 | 23.50 | 13.90 | 20.34 |
| 4 | 7–6 | 0.45 | 0.52 | 15.25 | 4.69 | 8.31 | 22.50 | 19.00 | 21.38 |
| 5 | 10–6 | 0.7 | 0.38 | 5.40 | −2.34 | 1.21 | 22.50 | 13.70 | 19.64 |
| 6 | 20–6 | 0.23 | 0.47 | 19.85 | 6.34 | 16.02 | 24.20 | 8.60 | 17.17 |
| 7 | 22–6 | 0.23 | 0.60 | 27.62 | 5.75 | 17.55 | 26.50 | 15.10 | 21.96 |
| 8 | 26–6 | 0.17 | 0.49 | 26.85 | 5.60 | 17.58 | 20.00 | 10.30 | 16.24 |
| 9 | 27–6 | 0.23 | 0.57 | 20.95 | 6.24 | 15.71 | 20.20 | 16.60 | 18.39 |
| 10 | 13–12 | 0.47 | 0.63 | 14.90 | 1.45 | 9.01 | 32.50 | 27.80 | 30.32 |
| 11 | 18–12 | 0.49 | 0.60 | 12.69 | 3.01 | 9.33 | 34.30 | 28.10 | 31.32 |
| 12 | 18–12 | 0.39 | 0.62 | 16.10 | −0.15 | 11.74 | 34.40 | 29.60 | 31.69 |
| 13 | 21–12 | 0.3 | 0.58 | 19.49 | 9.50 | 15.89 | 35.00 | 30.00 | 33.79 |
| 14 | 22–12 | 0.07 | 0.33 | 50.00 | 27.74 | 45.02 | 35.00 | 29.00 | 31.20 |

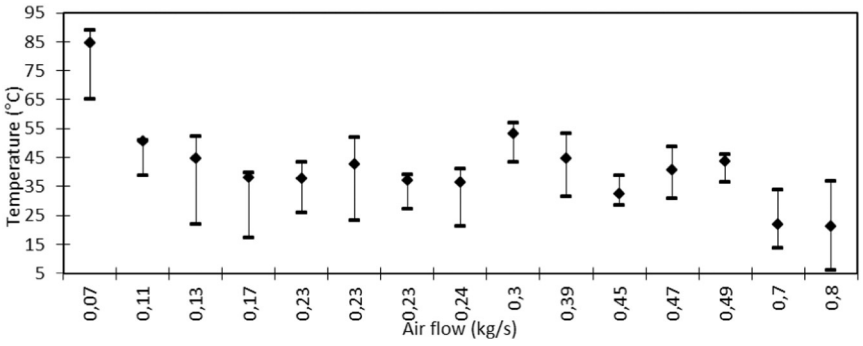


**Fig. 12.** Average temperature of the air flow at the outlet of collector.

where $\dot{m}$ is the mass air flow, $C_p$ is the air heat capacity and (Tout – Tin) is the difference of temperature according Eq. (3).

In Fig. 14 the behavior of the estimated useful power is shown. From this, a maximum of 7000 W with airflow between 0.45 kg/s and 0.47 kg/s was obtained, being the average around 3500 W.

The results of thermal efficiency versus air flow are shown in Fig. 15. The dots indicate the mean value of efficiency according to Table 2. A parabolic curve was obtained varying the air flow, whose polynomial fit, is represented with a solid line. The highest efficiency values 0.6 were obtained in an interval around 0.4 kg/s. As expected, low air flows led to low efficiency levels. By contrast, the highest air flow values did not lead to higher efficiency. If a more adequate drying output temperatures near to 50 °C are taken into account, an air flow of 0.23 kg/s was more convenient, being the efficiency only slightly lower than the highest value, that is 55%. Lower values of the airflow produced more hours of temperatures above 50 °C.

## Cost and revenue analysis

A cost analysis of the tested dryer was performed. The costs of construction and installation of a drying chamber, six carts, a master duct, a cabinet with air filters, an electric fan and a bank of 10 solar collectors were considered. Material and labour costs amounted to 8000 USD at 2008 prices in Salta city. The largest percentage of total costs (37%) correspond to the materials used for the collector array, 13% to the tunnel, 14% to the carts, 16% to the master duct while labour represents only 20% because local labour force from the cooperative, which is cheaper, was hired.

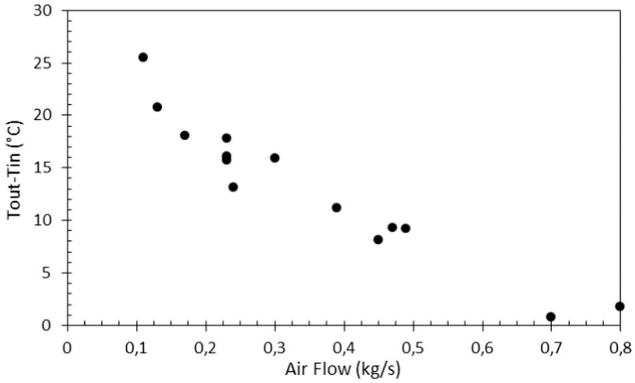


**Fig. 13.** Difference of temperature in the solar collector.

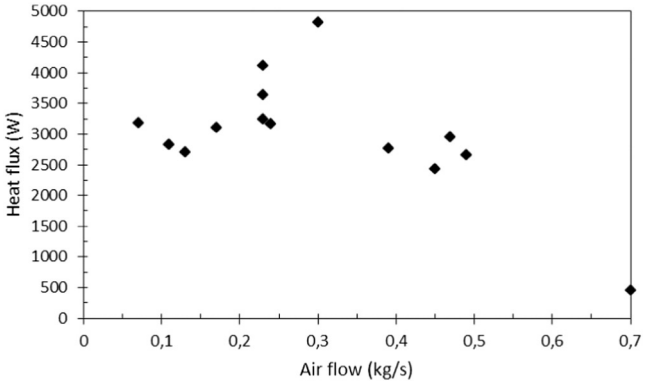


**Fig. 14.** Useful power delivered by the collector.

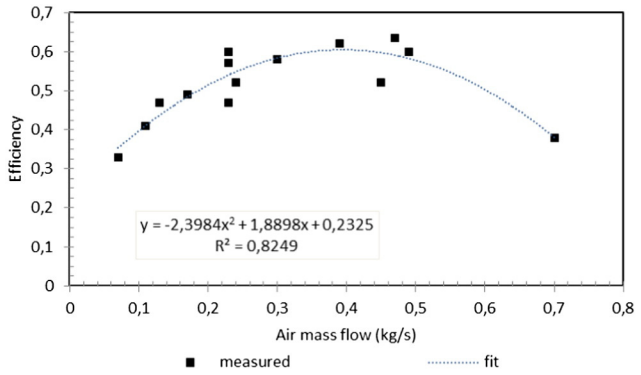


**Fig. 15.** Average thermal efficiency of collector versus the air flow in the collector.

The cost per square meter of collector was approximately USD 33, while for the drying chamber this cost was USD 45. As an alternative to reduce costs, the north side and roof of the drying chamber could be used as solar collectors. In this way, the total collector area and the chamber cost could be reduced by 20%.

Two scenarios were analysed, one related to the solar dryer proposed and the other related to an electrical dryer. The latter was only used for calculation and comparative analysis, since it was not constructed or used. However, since electricity is the only conventional energy available in the area, an electrical dryer would be a feasible option.

a) Conventional Scenario: the production process is done through an electrical drying system which demands 80.6 MWh to complete the annual production cycle.
b) Clean Energy Project Scenario: energy demand is fulfilled by the semi-industrial solar dryer. An annual electricity consumption of 2.68 MWh corresponds to an engine for air circulation.

The financial analysis was performed considering that the solar technological option involves no modification on the volume production of fresh product (15 ton) and on the final sale price of the dried product (USD 3/kg). The initial investment is different for the options studied since it is required a higher investment on the solar system due to solar collectors. Another difference is the annual labour cost because the solar dryer needs the cleaning and replacement of the collectors' transparent cover. The situation is similar for the production cost since the product management is diverse; on the solar system the product has to be moved from the dryer during night hours. Finally, the electrical heating has influence only on the electrical dryer. Paprika pepper production was taken as basis for the calculation of these indicators.

Several indicators were used for the financial assessment of dryers as an investment project: the net present value (NPV), the internal rate of return (IRR), the payback period (PB) and the benefit–cost ratio (BCR). An annual interest rate (IR) of 30%, corresponding to Argentina, was considered. According to the cash flow and considering the energy savings, the results indicate that the investment could be recovered in 13 months in the solar case and in 21 months in the electrical one.

A social assessment was also performed using the social net present value (SNPV) as indicator (Hirschey, 2009), considering the avoided externalities costs due to the GHG reduction and electricity prices. In this case, a social discount rate of 12% was used (this rate was taken from the Economic Planning Secretary of Argentina).

According to the information provided by the producers, the average annual production is around 120 tons, and the product is sold in the local market at a price of USD 3/kg of dried product. Taking the conditions of the domestic market into account it is expected that the price will not change in the short term.

The cost of electricity, for both scenarios, was calculated based on the average annual production and the local rate of electricity according to the consumption category (annual fixed cost of 70.08 USD and variable cost of 0.057 USD/KWh). The analysis horizon was defined in 4 years.

**Table 3**
Costs and revenues summary for the two scenarios analysed.

| | | Electrical dryer | Solar dryer |
|---|---|---|---|
| Costs | Initial investment | $5.333,33 | $8.000,00 |
| | Annual labour cost | $666,67 | $1.000,00 |
| | Fresh product annual cost (15 ton) | $33.000,00 | $33.000,00 |
| | Production cost | $3.000,00 | $3.333,33 |
| | Electrical engine | $190,67 | $190,67 |
| | Electrical heating | $5.227,40 | $– |
| | Fixed costs | $70,07 | $70,07 |
| Revenues | Sale of dried product | $45.000,00 | $45.000,00 |

**Table 4**
Financial and social indicators for conventional and clean energy project scenario.

| | Conventional | Clean Energy Project |
|---|---|---|
| NPV | USD 1807 | USD 9733 |
| IRR | 43% | 88% |
| BCR | 1.27 | 4.25 |
| PB | 21 months | 13 months |
| SNPV | USD −205 | USD +34,856 |

Based on the indicators obtained, both scenarios are financially feasible (NPV ˃ 0 and IRR > IR), but only the clean energy project is feasible from a social-environmental point of view (SNPV > 0) (Table 3). The clean energy project scenario shows an improvement of the financial indicators of 438% when compared with the conventional scenario (Table 4).

## Conclusions

An indirect forced-air flow solar dryer was built in northern Argentina, using an array of large solar collectors. The chamber, opaque to solar radiation, allowed the drying of a wide variety of vegetables. The use of trays and carts made the handling of products in the chamber easier. The structure was resistant to the strong winds of the zone. The slope of the collectors might be oriented according to the solar noon altitude, optimizing the annual collector efficiency.

The solar collectors allowed the dryer to operate with temperatures around 50 °C for 6 or 7 h considering a sunny day. In this case, the air flow was 0.07 kg/s, and the air coming from the collectors was mixed with ambient air to lower the temperature in the drying chamber. The dryer was regularly tested with different vegetables in different seasons of the year, showing a satisfactory performance. The dried product obtained had good final moisture content and was free of dust pollution. Dryer efficiency varied between 30% and 40%.

From the solar collector prototype tests, the maximum collector efficiency was around 0.6, with 0.4 kg/s of air flow. A close range was near to 50 °C with an air flow of around 0.23 kg/s, obtaining a useful heat flux of 4000 W and a thermal efficiency near to 55%. Consequently, around 2 kg/s of air flow are required by the entire collector bank. For flows of 0.07 kg/s the efficiency of collectors falls to about 30%.

The solar collectors' bank provided enough energy to dry 450 kg of fresh product during 16 h of sun. However, the measures showed that the useful energy of the collectors was not fully employed. Some corrections were applied from the original model to improve the air distribution and temperature between trays. Among these corrections, screens were put around the carts. Thermal losses were detected since the temperatures drop around 13 °C between the collector output and the drying chamber entrance.

If the dryer is considered as a clean energy project and compared with a traditional case that uses electric power, the investment return rate would be reduced from 21 to 13 months. The efforts to improve

the collector's efficiency might have an important impact on the dryer cost. It is possible to reduce the area of collectors and to reduce the cost of the drying chamber by 20%. The scenario with clean energy project improves the NPV in a 438% and the SNPV indicates the social-environmental feasibility only for the clean energy project.

## References


Altobelli F, Condorí M, Durán G, Martínez C. Solar dryer efficiency considering the total drying potential. Application of this potential as a resource indicator in northwestern Argentina. Sol Energy 2014;105:742–59.

Belmonte S, Núñez V, Viramonte J, Franco J. Potential renewable energy resources of the Lerma Valley, Salta, Argentina, for its strategic territorial planning. Renew Sustain Energy Rev 2009;13:1475–84.

Condorí M, Echazú R, Saravia L. Secador solar indirecto con flujo de aire forzado para Huacalera, Quebrada de Humahuaca. Avances en Energías Renovables y Medio Ambiente 2006;10:02.47–54.

Duffie JA, Beckman WA. Solar engineering of thermal processes. 3rd ed. New York: Wiley; 2006.

Echazú R, Condorí M, Saravia L. Curvas de Secado experimentales en la planta de deshidratado solar de Huacalera. Avances en Energías Renovables y Medio Ambiente 2007;11:02.09–16.

Ekechukwu OV, Norton B. Review of solar-energy drying systems III: low temperature air-heating solar collectors for crop drying applications. Energy Convers Manag 1999;40:657–67.

Hirschey M. Fundamentals of managerial economics. 9th ed. Ohio: South-Western Cengage Learning; 2009.

Mujundar A, editor. Handbook of industrial drying. New York: Marcel Dekker Inc.; 1987.

Reghini R, Grossi Gallegos H, Raichijk C. Approach to drawing new global solar irradiation contour maps for Argentina. Renew Energy 2005;30:1241–55.

Ringeisen B, Barret D, Stroeve P. Concentrated solar drying of tomatoes. Energy Sustain Dev 2014;14:47–55.

Sharma A, Chen CR, Lan NV. Solar-energy drying systems: a review. Renew Sustain Energy Rev 2009;13:1185–210.

Soponronnarit S. Solar drying in Thailand. Energy Sustain Dev 1995;2:19–25.

Stiling J, Li S, Stroeve P, Thompson J, Mjawa B, Kornbluth K, et al. Performance evaluation of an enhanced fruit solar dryer using concentrating panels. Energy Sustain Dev 2012;16:224–30.

VijayaVenkataRamana S, Iniyanb S, Ranko G. A review of solar drying technologies. Renew Sustain Energy Rev 2012;16:2652–70.